GLL
Geomatics, Landmanagement and Landscape No. 2 • 2024, 67–83

ISSN 2300-1496 http://dx.doi.org/10.15576/GLL/2024.2.05

Research paper

Received: 18.12.2023
Accepted: 24.03.2024
Published: 31.07.2024

Mapping of annual and frequency rainfall in the Cheliff catchment area (Northwestern Algeria)

Mohamed-Sadek Messis[1, ✉] 0009-0009-0851-7999
Azeddine Mebarki[1] 0009-0005-7519-1846
Abdelaaziz Merabti[2] 0000-0001-8611-0793

[1] Department of Territory Planning, Faculty of Earth Sciences, Geography and Territory Planning, Constantine 1-Frères Mentouri University, Laboratory of Territorial Sciences, Natural Resources and the Environment (LASTERNE)
[2] Laboratory of Preservation and Protection of Water Resources, Department of Water Sciences and Environment, University of Saad Dahlab Blida 1, Algeria
✉ Corresponding author: mohamedsadek.messis@doc.umc.edu.dz

Summary

In recent years, there has been a common use of automatic precipitation mapping based on various interpolation methods. Based on multiple linear regression, the study primarily focuses on the entire Cheliff basin (43 750 km²), to search a suitable model for mapping mean annual precipitation based on 89 rainfall stations of the observed series (1968/69–2001/2002). Then conducts on the upper part of Cheliff basin downstream the Boughzoul dam (4777 km²) using 11 rainfall stations of annual precipitation series relative to the period 1982/83–2020/2021. The same approach was used to map median annual precipitations and quantiles of rain associated with the return periods of 5 and 10 years, representing both wet and dry periods. Indeed, this work is based on the backward elimination method between the observed annual precipitation and four predictors: smoothed altitude (Z_s), longitude (X), latitude (Y) and distance from the sea (D). The model's results are satisfactory with a global correlation coefficient for both regional (R = 0,89) and local scale (R > 0,81). The final maps obtained are produced after interpolating by kriging the residuals. The median annual precipitation map was compared to that elaborated by the National Hydraulic Resources Agency (ANRH). The comparison results of 2296 nodes of the grid covering the Upper Cheliff basin showed negative deviations on average − 10% and reaching − 34% in northern area reflecting a dry trend in precipitation. The final grids of rainfall can be integrated into Geographical Information Systems related to many sectors including water management and climate change.

Keywords

rainfall • relief parameters • multiple linear regression • automatic mapping • Cheliff

1. Introduction

Automatic mapping can serve as a process for estimating precipitation at each location within various regions. It is often used to produce precipitations maps for several contexts in the world. For example, the geostatistical method well known as kriging, and the multiple linear regression method (MLR), are used in various geospatial analyses and cartography, particularly for mapping climate parameters. It is of utmost important for water resources management to have the necessary knowledge about climatic parameters such as precipitation. Geostatistical method does not consider the physical characteristics of the region and requires many rainfall stations. It also gives inaccurate values on mountain tops [Traboulsi 2010]. However, the MLR method considers all the environmental parameters that could be explanatory. Hence [Laborde 1982, Assaba and Laborde 2000, Laborde et al. 2003, Mebarki 2003, Louamri 2009] have used the MLR method by adding the error map interpolated by kriging after validation of a variogram model. Many studies have been conducted using MLR method, Laborde [1982] developed the method by using it to cartography the maximum daily precipitation in the north-eastern of France. Chutsagulprom et al. [2022] compared three methods (Artificial Neural Networks (ANN), MLR, inverse distance weighting, inverse exponential weighting, and ordinary kriging) to cartography a monthly precipitation in Thailand and have shown that ANN was less efficient than the other methods. Several researchers used MLR method across the Mediterranean basin, Assaba and Laborde [2000] employed MLR in the region of Corsica in France to cartography monthly precipitation. Using same process Zahar and Laborde [2008] have linked morphometric parameters to extreme daily precipitation in Tunisia. Bostan et al. [2012] compared different interpolation methods in Turkey and concluded that the universal kriging method and the MLR method yield very good interpolation results. In Algeria, the producing map by A.N.R.H. [1993] of interannual average precipitation on a scale of 1:500,000 over a period of 60 years (from 1st September 1921 to 31 August 1960 and from 1st September 1968 to 31 August 1989), is the first map product in Algeria using the numerical method. Using the classical mapping methods, annual precipitations maps were produced by Seltzer [1946] at a scale of 1/1000000 covering the period 1913–1938, Gaussen [1948] at a scale of 1/500000 covering the period 1913–1947 and Chaumont and Paquin [1971] at a scale of 1/500000 covering the period 1913–1963.

Then, several studies have been elaborated on the digital mapping of rainfall in Algeria for different purposes. Mebarki [2003] used the MLR method to map the median annual rainfall in the north-east of Algeria for the period 1972/73–1983/84 and then integrated the product into the estimate of surface runoff after calculating the runoff deficit of the basin, which in turn was mapped [Mebarki 2010]. Louamri [2009] produced a map of median rainfall in the Seybouse catchment area over the period 1969–1998 by relating the precipitation with smoothing altitude and distance

to the sea. Bénina et al. [2006] mapped mean annual, dry ten-year and dry five-year rainfall in north-central Algeria. Laborde et al. [2003] produced maps on a monthly scale, even for a particular month, for the whole of northern Algeria by relating median rainfall and its standard deviation, they based their maps on the interpolation of Gauss variables. Other studies, such as those by Benali Khodja et al. [2022] have used the geostatistical method (kriging) without integrating environmental parameters to map annual rainfall in the Oued Isser catchment area.

Based on MLR method, the study primarily focuses on the entire Chellif basin (43 750 km²), to search an appropriate model for mapping annual average precipitation based on 89 rainfall stations across the period from September 1968 to August 2002. Then conducted on the upper part of Chellif basin downstream the Boughzoul dam (4777 km²) using observed series (1982/83–2020/21) of 11 stations. The same approach was adopted for mapping both of median annual rainfall and annual frequency rainfall associated to return periods of 5 and 10 years.

Indeed, this work is based on the backward elimination method between the observed annual precipitation (variables to be explained) and explanatory variables using 'HYDROLAB 2018' which is a programme developed by Laborde et al. [2018]. It should be noted that Chellif basin is one of the richest basins areas in terms of water resources in Algeria [ABH-CZ 2004, 2007], with more than 1000 $Hm^3 \cdot year^{-1}$ of surface water available [Mebarki et al. 2013]. It provided water for various uses with 17 dams with a total capacity of 2320 Hm^3 [Hallouz et al. 2020]. The management of this resource requires a deep knowledge of climatic parameters such as precipitation.

2. Background, data, and methods

2.1. Study area

The Cheliff watershed, the largest basin in northern Algeria (43 750 km²), is under the influence of a semi-arid climate [Hallouz et al. 2020] (Fig. 1).

The Upper Cheliff downstream the Boughzoul dam (located in the north-east of Cheliff basin) covers an area of 4777 km², bounded by two mountain ranges, the Zaccar mountains to the north and the Ouarsenis mountains to the south of the region. The relief varies from 250 m (Khemis Miliana plain) to over 1600 m (Ouarsenis mountains). It is characterized by wet, relatively cold winters and hot, dry summers [Fellag et al. 2021]. An irrigation system was inaugurated in 1941 and is actually supplied by three dams (Ghrib, Deurdeur and Harezza) with a capacity of 280 Hm^3, 115 Hm^3 and 75 Hm^3 respectively [ONID 2020].

2.2. Data

Relating the regional approach (the Cheliff basin), we used the interannual precipitation data covering the period of September 1968 to August 2002 after selected 89 rainfall stations from ABH-Cheliff-Zahrez synthesis study [ABH-CZ 2004, 2007] (Fig. 1). Relating the upper Cheliff area in the north-east of Cheliff, we have treated the monthly

and the annual precipitation data of eleven (11) rainfall stations from the database of the National Hydraulic Resources Agency (ANRH) and the National Institute of Field Crops (ITGC). These observed series are covering a common period from September 1982 to August 2021.

The Digital Elevation Model (DEM) data, with a 2 km × 2 km mesh covering the Cheliff catchment area, were extracted from a satellite image covering the entire African continent (EROS Data Center of the U.S. Geological Survey).

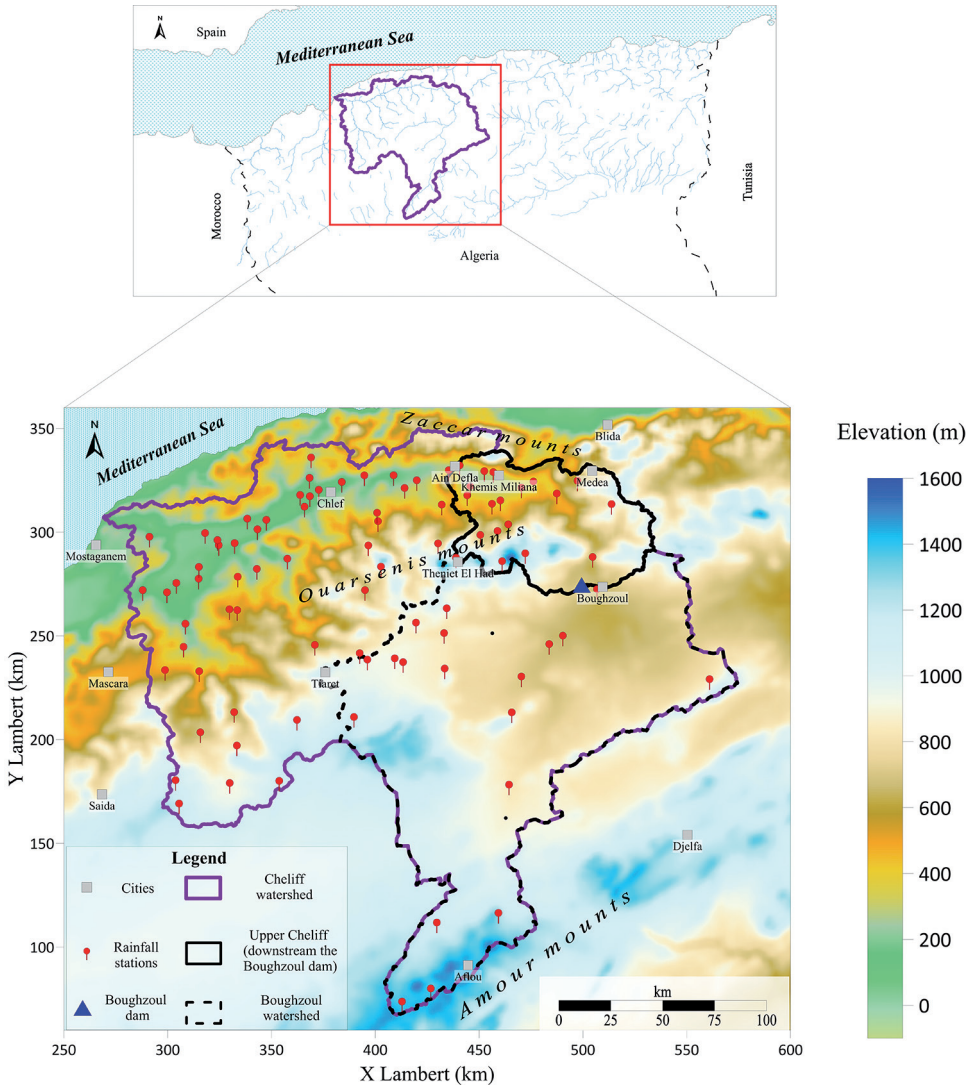

Source: Author's own study

Fig. 1. Presentation of the study area

2.3. Methods

2.3.1. Data processing

Mapping on a regional scale in the Cheliff catchment area is made of mean annual rainfall data extracted directly from ABH-Cheliff-Zahrez synthesis study.

The annual rainfall data from the 11 stations of upper Cheliff is fitted to the normal root distribution function, also used by Laborde [1995]. Characterised by two parameters, the mean of the square roots of the rainfall series ($\overline{\sqrt{P}}$) and the standard deviation of the square roots of the rainfall ($\sigma\sqrt{P}$), the distribution function of the root law is given:

$$F(x) = \frac{1}{\sqrt{2\pi}} \int_{-\infty}^{u} e - \frac{u^2}{2} du \tag{1}$$

with:

$$u = \frac{\sqrt{P} - \overline{\sqrt{P}}}{\sigma\sqrt{P}}$$

where:

$F(x)$ – the probability that any value of X is less than or equal to x,
u – the standardized Gaussian variable.

This step was checked using the Anderson test U(%) of Anderson and Darling [1952].

The homogeneity of the data from 11 rainfall stations was tested using the sequential Wilcoxon test [Karl and Williams 1987].

Then the rainfall variables are root-transformed ($\sqrt{P_i}$), and estimated the frequential rainfall for each return period: 2-year return period ($\overline{\sqrt{P}}$), the return period of dry years ($\sqrt{P_{F0.1}}$ and $\sqrt{P_{F0.2}}$) and the return period of wet years ($\sqrt{P_{F0.8}}$ and $\sqrt{P_{F0.9}}$). The followed equation is the basis for the frequency values:

$$\left(\sqrt{P_F} = u \cdot \sigma\sqrt{P} + \overline{\sqrt{P}}\right) \tag{2}$$

The five-year and ten-year frequencies are important in water resource management studies, particularly for irrigation water supply [A.N.R.H. 1993, Bénina et al. 2006, Le Mezo 2013].

2.3.2. Multiple linear regression (MLR)

The multiple linear regression (MLR) used as a statistical approach to produce rainfall maps, which is a common method estimates the variable to be explained at each observed point from several explanatory variables (X_1, X_2, X_3, …, X_j). The equation is given below:

$$Y_i = a_1 X_1 + a_2 X_2 + a_3 X_3 + ... + a_j X_j + a_0 + \varepsilon \tag{3}$$

where: a_j, a_0 and ε are the multiple regression coefficient, the constant and the estimation errors (residuals), respectively.

The 'backward elimination' method, explained by Laborde et al. [2018], involves validating the explanatory variables using two validation tests with a significance threshold α = 5%. The first one is the Fisher Snedecor test (F test), which considering that the global correlation coefficient (R) is significant if the variance explained is significantly greater than the residual variance (4). The second test is the Student's t test, considers the partial correlation coefficient (r_i) in its lowest absolute value (5). If at least one of the two tests rejects the hypothesis of independence, the variable with the lowest partial correlation coefficient will be removed and the multiple regression repeated with one less explanatory variable.

$$F = \frac{n-(k+1)}{k} \cdot \frac{R^2}{1-R^2} \tag{4}$$

$$t = \frac{r^2}{\sqrt{\frac{1-r^2}{n-2}}} \tag{5}$$

where:

n – sample size,

k – number of explanatory variables.

The above calculations were made using the 'HYDROLAB' software [Laborde et al. 2018].

The relief variables considered as potentially explanatory factors are extracted for each station from the data presented in the form of a grid: smoothed altitude (Z_s in meters), longitude (X Lambert North Algeria given in meters), latitude (Y Lambert North Algeria given in meters) and distance from the sea (D given in meters), using the 'Point Sample' tool on the SURFER 25 software [Surfer® 2023]. These variables can affect the rainfall geographical distribution in the northern region of Algeria, as defined in previous works [Laborde 1995].

The advantage of the Smoothed Altitude variable is to account the terrain, which may have an impact on the movement of air masses [Laborde 1982] and eliminate roughness from the digital elevation model [Van Nieuwenhuizen et al. 2021]. The spatial resolution chosen (2 km × 2 km) means that landforms likely to influence rainfall distribution are correctly represented [Laborde 1995].

The distance to the sea variable (D) is estimated, for each point in the selected space, by the following equation:

$$D = \min\sqrt{\left(X_i - X_c\right)^2 + \left(Y_i - Y_c\right)^2} \tag{6}$$

where:

X_i and Y_i – the geographical coordinates of a point in the study area [m],

X_c and Y_c – the geographical coordinates of points on the coastline [m].

2.3.3. Interpolation of residual values

According to Laborde [1995], the residuals have a mean of zero and constant variance. They vary with spatial position and are readily amenable to interpolation. The estimation error map (ε) is obtained from spatial interpolation using the geostatistical method (kriging). The best fitted theoretical variogram model is validated using the root mean square error RMSE [Willmott and Matsuura 2006] taking the lowest value.

$$RMSE = \sqrt{\left[\frac{1}{N}\sum_{i=1}^{N}\left(xi - yi\right)^2\right]} \tag{7}$$

where:

xi – the observed variable (error calculated by $\sqrt{P} = \sqrt{Pest} + \sqrt{\varepsilon}$),
yi – the estimated error variable by the model.

The scheme summarises the method of rainfall mapping applied on upper Cheliff (Fig. 2).

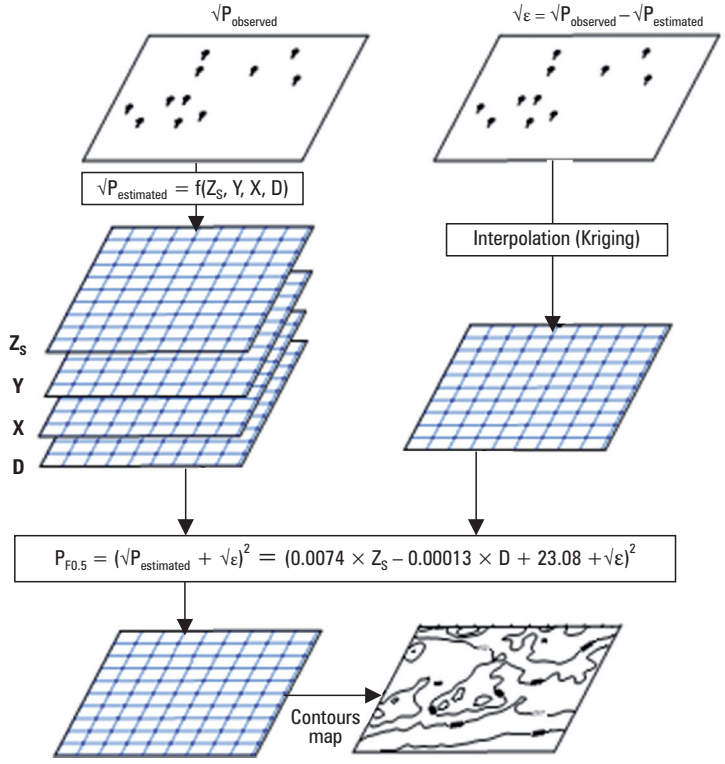

Source: Authors' own study

Fig. 2. Automatic mapping method

3. Results and discussion

3.1. The mean annual rainfall map of the Cheliff catchment area (1968/69–2001/02)

The Table 1 summarises the results after applying multiple regression to 89 stations distributed across the catchment. The validated multiple regression model includes four explanatory variables (Z_s, YZ_s, Y and X) with an overall correlation coefficient of R = 0.89. The latitude (Y) is the most influential factor on the spatial variation of rainfall with a partial correlation coefficient (r_i = 0.757), followed by longitude (X) with a negative partial correlation coefficient (r_i = −0.597) then the smoothed altitude (Z_s) with r_i = 0.544 and finally the product of smoothed altitude and latitude (YZ_s) with r_i = −0.26. The two variables longitude (X) and the product of latitude and altitude (YZ_s) have an inverse relationship with the spatial variation of rainfall. The final calculation for the mean annual rainfall map is as follow:

$$P_{est}\,(\text{mm}) = 0.4085 \cdot \text{Zs} - 0.000537 \cdot 10^{-3} \cdot \text{YZs} + 0.00280 \cdot \text{Y} - 0.00063 \cdot \text{X} - 326.20 + \varepsilon \quad (8)$$

Table 1. Multiple regression results for the Cheliff catchment area

Explanatory variables	a_i	r_i	a_0	R	F Fischer Sedecor	t Student
Z_s [m]	0.4085	0.544	−326.20	0.89	0.00%	1.60%
YZ_s [m × m]	$-0.000537 \cdot 10^{-3}$	−0.26				
Y [m]	0.00280	0.757				
X [m]	−0.00063	−0.597				

The parameter $\varepsilon = P_{obs} - P_{est}$ is the residual of the estimated rainfall at each point of the grid. The residuals are mapped using the 'Ordinary Kriging' interpolation method, whose best validated variogram model is the spherical model with RMSE = 38.72 (Table 2).

Table 2. Validation parameters of the variogram model (spherical) for the mean annual rainfall map (1968/69–2001/02).

Range [km]	35.57	Partial Sill	1609
Anisotropy	1.913	Angle [°]	162.9
RMSE	38.72	Nugget	0

In general, the variation in mean annual rainfall in the Cheliff catchment decreases from north (700 mm) to south (100 mm) (Fig. 3). The values are higher in the Zaccar and Ouarsenis mountains in the north of the basin (400 to 700 mm). However, in the western

part of the catchment, mean rainfall varies from 250 mm in the wadi Mina to 400 mm in the south of Chlef city. In the south-east, precipitations are low (below the 300 mm curve) peculiarly in the upstream part of the Boughzoul dam. According to Capot-Rey [1946], the variability of the rainfall depends on the activity of the fronts separating the polar and tropical air masses, which diminishes from north Africa towards the Sahara. This explains the decrease in the amount of precipitation from north to south.

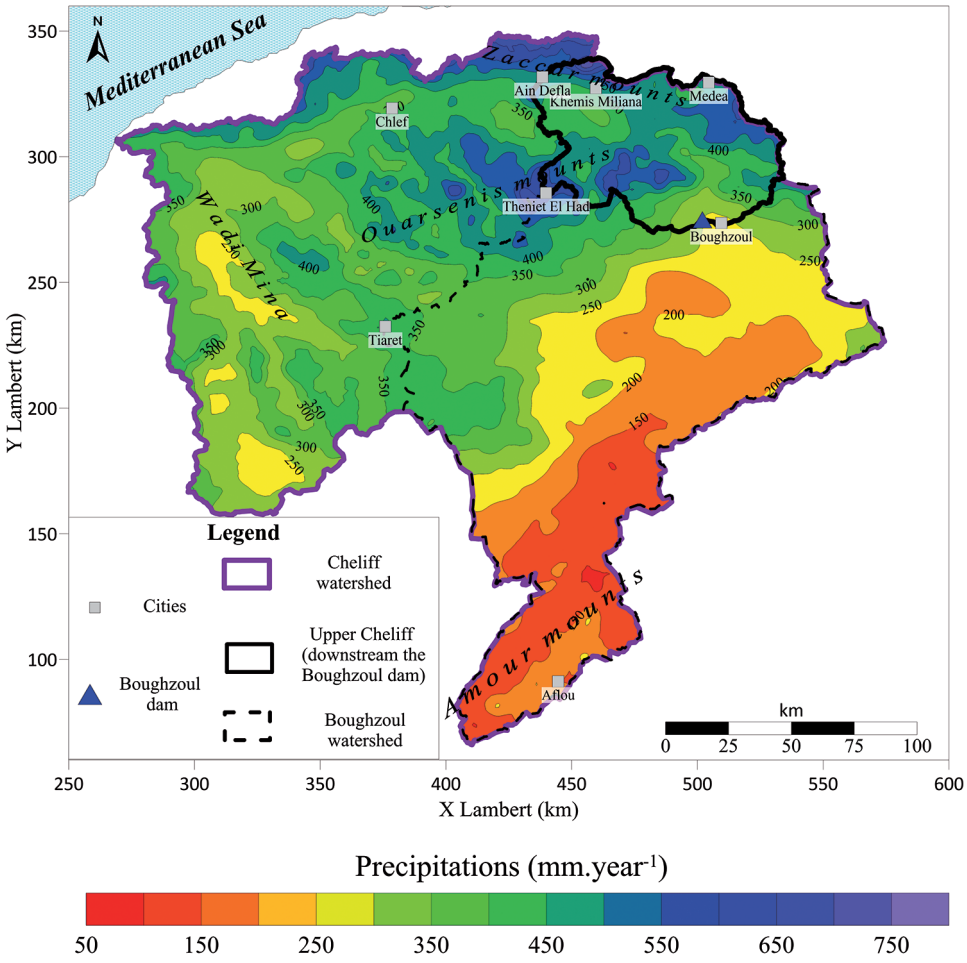

Source: Authors' own study

Fig. 3. Mean annual rainfall in the Cheliff catchment area (September 1968–August 2002)

3.2. Mapping of the annual frequency rainfall in Upper Cheliff region

On this stage, we mapped the median annual rainfall ($P_{F0,5}$) and the quantiles of rain associated with the return periods of 5 and 10 years (wet periods: $P_{F0,8}$ and $P_{F0,9}$ and dry

periods: $P_{F0,1}$ and $P_{F0,2}$). At the local scale, the number of validated explanatory variables decreased compared to the regional scale. The two variables validated by the calculation programme are smoothed altitude (Z_s) and distance to the sea (D), whatever the frequency, with the change in the regression coefficients for each explanatory parameter a_i (a_1, a_2) and the constant a_0 (Table 3). The global correlation coefficient registered for the mean roots' rainfall reached the value of 0.878. For the frequency values R varied from 0.81 to 0.86. The rainfall is related to altitude (Z_s), the main factor influencing rainfall, with a value of r_i close to the overall correlation coefficient R. The distance from the sea (D), second only factor to the Z_s, is inversely related to rainfall amount (Table 3).

Table 3. Explanatory variables for frequent annual rainfall estimated by the multiple regression method

	Parameter $\sqrt{P_F}$ [mm]	Equation: $\sqrt{P_F} = a_1Z_s + a_2D + a_0$	R	r_i		F [%]	t [%]
				Z_s [m]	D [m]		
Dry period	$\sqrt{P_{F0.1}}$	$0.0061 \cdot Z_s - 0.00010 \cdot D + 18.81$	0.818	0.817	−0.763	1.20	1.00
	$\sqrt{P_{F0.2}}$	$0.0066 \cdot Z_s - 0.00011 \cdot D + 20.28$	0.855	0.854	−0.808	0.50	0.50
Median	$\sqrt{P_{F0.5}}$	$0.0074 \cdot Z_s - 0.00013 \cdot D + 23.08$	0.878	0.878	−0.836	0.30	0.30
Wet period	$\sqrt{P_{F0.8}}$	$0.0082 \cdot Z_s - 0.00014 \cdot D + 25.89$	0.86	0.859	−0.813	0.50	0.40
	$\sqrt{P_{F0.9}}$	$0.0087 \cdot Z_s - 0.00015 \cdot D + 27.36$	0.842	0.841	−0.791	0.29	0.23

The finale equations are given by $P_F = (a_1Z_s + a_2D + a_0 + \sqrt{\varepsilon})^2$ after mapping the residuals $\sqrt{\varepsilon} = \sqrt{P_{Fobs}} - \sqrt{P_{Fest}}$ using the 'ordinary kriging' interpolation method with linearly variogram model.

The final maps covering 2296 nodes of the grid, illustrate the median annual rainfall, ten-year and five-year dry rainfall, and ten-year and five-year wet rainfall (Fig. 4, 5, 6). The median rainfall (2-year return period) for the whole region is 413 mm, decreasing to 200 mm towards the south and reaching a maximum of 730 mm in the north-west (Monts du Zaccar). On the Ech Chaoun mountains, rainfall starts at 450 mm and exceeds 550 mm on the summits. The curve of 400 mm crosses the Khemis Miliana city in the north-west of the region.

According to Figure 5, the ten-year dry rainfall varies from about 120 mm in the south to 500 mm in the north-western mountains of Khemis Miliana city, between 250 mm and 300 mm in the centre of the region and over 300 mm in the Ech Chaoun mountains. The five-year dry rainfall map shows a slight increase of about 50 mm compared to the ten-year dry rainfall (Fig. 6).

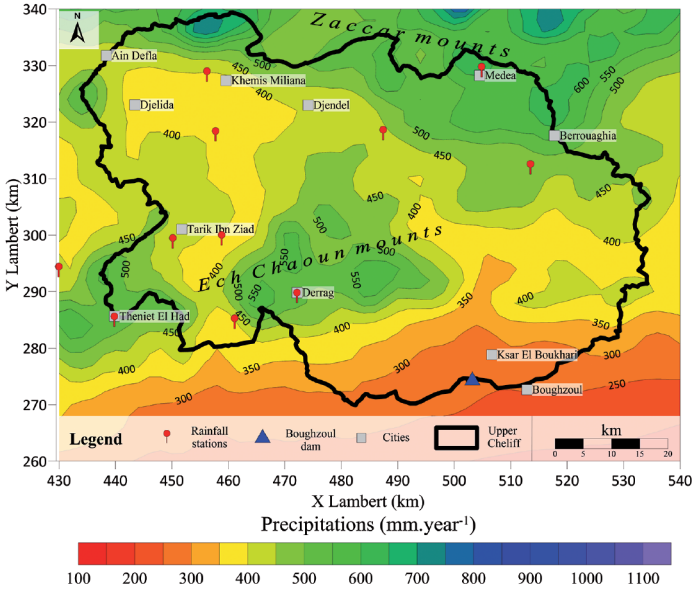

Source: Authors' own study

Fig. 4. Median annual rainfall in the Upper Cheliff (north-east of Cheliff basin) (September 1982–August 2021)

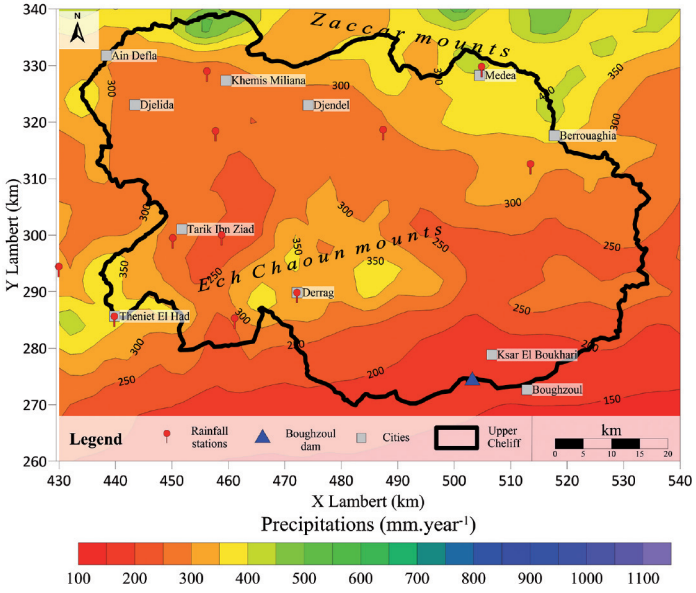

Source: Authors' own study

Fig. 5. Rainfall frequency maps for ten-year dry rainfall ($P_{F0,1}$)

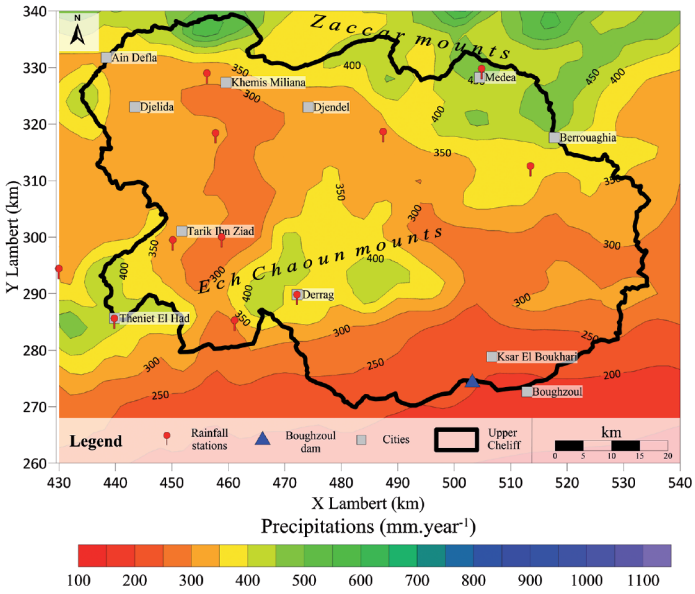

Source: Authors' own study

Fig. 6. Rainfall frequency maps for five-year dry rainfall ($P_{F0,2}$)

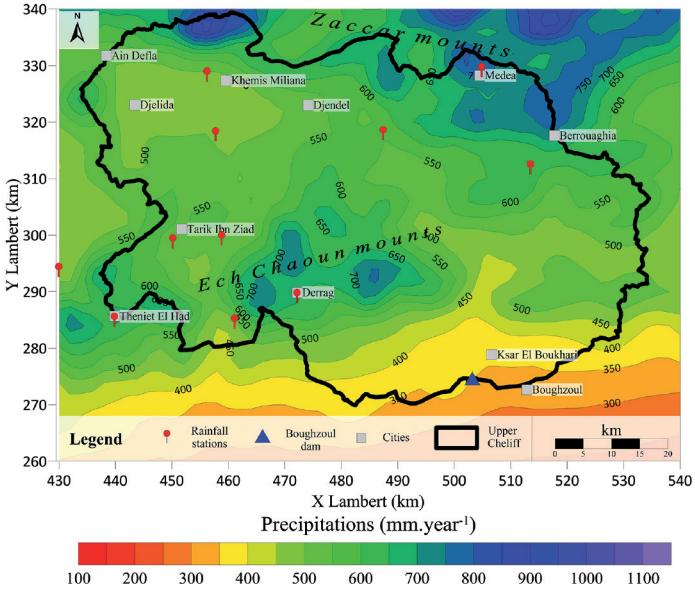

Source: Authors' own study

Fig. 7. Rainfall frequency maps for five-year wet rainfall ($P_{F0,8}$)

The spatial variability of rainfall in both wet and dry years is notable. Five-year wet rainfall varies from 250 mm in the south-east to 1000 mm in the summits of Zaccar mountains in the north, while in the centre of the region it is between 500 and 600 mm and over 700 mm in the summits of the Ech Chaoun mountains (Fig. 7). The ten-year wet rainfall varies from 300 mm in the south to 1100 mm in the north, a difference of about 50–100 mm compared to the five-year wet rainfall (Fig. 8).

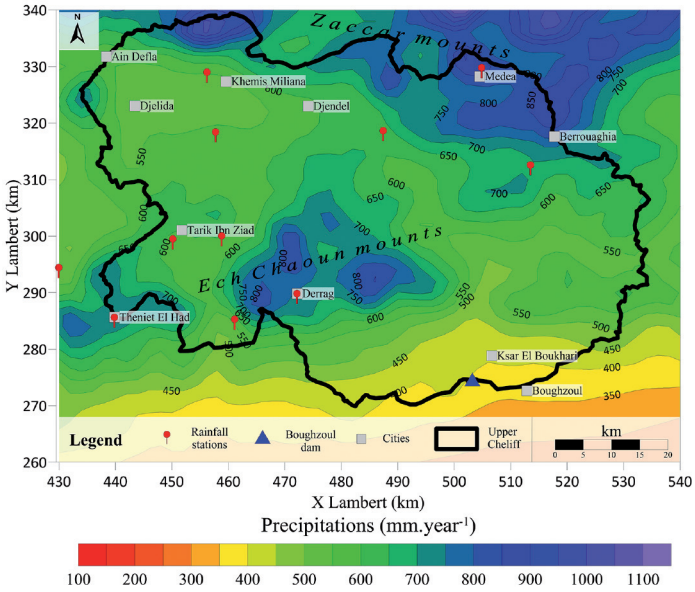

Source: Authors' own study

Fig. 8. Rainfall frequency maps for ten-year wet rainfall ($P_{F0,9}$)

Dry/wet variability, in the north of Algeria, depends on variability in general atmospheric circulation models such as North Atlantic Oscillation (NAO), El Niño Southern Oscillation (ENSO), Mediterranean Oscillation (MO) and Western Mediterranean Oscillation [Tramblay et al. 2013, Taibi et al. 2017, Boutouatou 2020, Hallouz et al. 2020, Zerouali et al. 2021].

3.3. Comparison of the median rainfall with the ANRH map

The median annual rainfall results, obtained over the 2296 nodes of the upper Cheliff region (period 1982/83–2020/21), are compared with the median annual of ANRH map for a reference period (1921–1960 and 1968–1989) [A.N.R.H. 1993]. Figure 9 shows the differences in rainfall. An average rainfall deficit of -10% is estimated for the period 1982/83–2020/21. This is due to the frequency of drought years between 1990 and 2002 [Taibi et al. 2013, Merabti 2018, Amiar et al. 2020, Mirgol et al. 2022]. Deficits were

observed over most of the study area, reaching − 34% in the north (Fig. 9). However, an increase in rainfall was observed in the extreme south of the region.

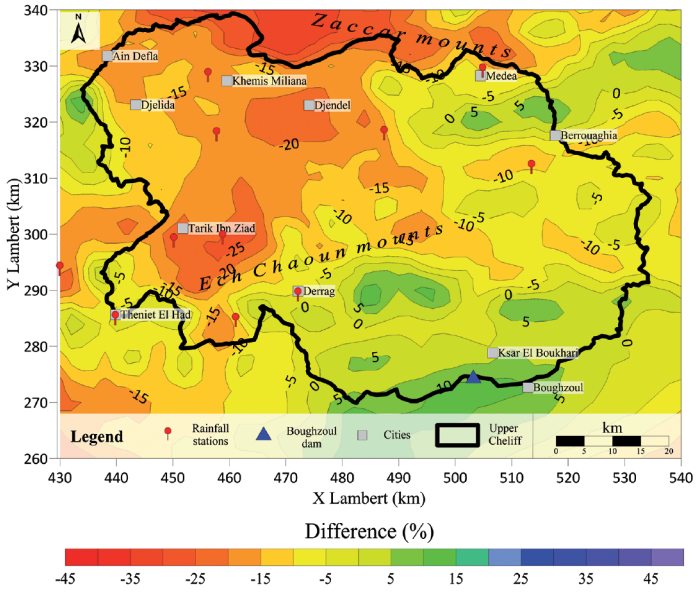

Source: Authors' own study

Fig. 9. Difference [%] in median annual rainfall (September 1982 and August 2021) compared to the ANRH map

The results of comparison with ANRH map concord with those found by Mebarki [2003] in the North-East of the country (−10%) over the period 1972/73−1983/84, as well as that detected by Louamri [2009] in the Seybouse basin (−10%) over the period 1969/70 to 1997/98. They also agree with the study of Meddi et al. [2014] in the North-West of the country (−13%) over the period 1968−1998. According to Assaba et al. [2013], surface runoff can be reduced by up to 45% with a 15% reduction in rainfall. The results of trend agree with the study elaborated by Zerouali et al. [2022], who found that the north-western region of Algeria was affected by a long-term dry period especially between 1980 and 2000. However, other methods can be used to diagnose more rainfall series behaviour.

4. Conclusions

The method used (multiple regression) to map the biennial ($P_{F0.5}$), ten-year dry ($P_{F0.1}$), five-year dry ($P_{F0.2}$), five-year wet ($P_{F0.8}$) and ten-year wet ($P_{F0.9}$) rainfall frequencies highlight the high relationship between annual rainfall and explanatory environmental variables. Based on the knowledge of these variables in the form of gridded data, rainfall can be estimated for each point in area. The method is applicable across various climate conditions, including the Mediterranean region. The method is versatile

and can be implemented across different scales by adjusting the explanatory variables. However, it is also appropriate to complement this method with other interpolation techniques, such as machine learning.

The 'backward elimination' method is used to validate, at the regional scale, four explanatory variables (smoothed altitude, latitude, longitude and product of smoothed altitude and latitude) with different weights. In addition, at the local level, two explanatory variables (smoothed altitude and distance from the sea) are validated. The final rainfall maps were obtained after mapping the residuals between observed and estimated rainfall using the geostatistical method (ordinary kriging). The mean annual rainfall in the Cheliff basin varies from 100 to 700 mm. In the upper Cheliff downstream of Boughzoul dam, the median rainfall varies from 200 mm in the south to about 730 mm in the north. In comparison with ANRH rainfall map, rainfall deficit, for the period 1982–2021, was estimated to average −10%. The results of frequency rainfall study, shown that rainfall reaches 1100 mm per year in the summits of mountains in the wet years and does not exceed 550 mm in dry years. The spatial variability of rainfall increases in wet years compared with dry years.

The rainfall maps obtained in grid form can be integrated into a geographic information system (GIS). This is a necessary tool for planning and managing water resources in a context of climate change.

References

ABH-CZ. 2004. Cadastre Hydaulique du bassin hydrographique du Cheliff-aval du barrage Boughzoul [Synthèse]. Agence de Bassin Hydrographique Cheliff-Zahrez.

ABH-CZ. 2007. Cadastre Hydaulique du bassin hydrographique du Cheliff-amont du barrage Boughzoul [Synthèse]. Agence de Bassin Hydrographique Cheliff-Zahrez.

Amiar S., Bouanani A., Baba-Hamed K., Belarbi H. 2020. Variabilité pluviométrique dans le bassin versant du Haut et Moyen Cheliff. Revue des Sciences de l'Eau, 32,4, 337–347. https://doi.org/10.7202/1069569ar

Anderson T.W., Darling D.A. 1952. Asymptotic Theory of Certain „Goodness of Fit" Criteria Based on Stochastic Processes. The Annals of Mathematical Statistics, 23,2, 193–212. https://doi.org/10.1214/aoms/1177729437

A.N.R.H. 1993. Carte pluviométrique de l'Algérie du Nord au 1/500000 (2 feuilles, une notice de 49 p.). Ministère de l'Equipement, éd. I.N.C., Alger.

Assaba M., Laborde J.-P. 2000. La prise en compte du relief dans l'estimation des pluies mensuelles: Le cas de la Corse. http://geoprodig.cnrs.fr/items/show/195057.

Assaba M., Laborde J.-P., Rezak S. 2013. Impact of a decrease in rainfall on regularized volumes by dams of Algeria. Le 5e Colloque International sur Ressources en Eau et Développement Durable (CIREDD), LJEE N° 21 et 22, 10–19.

Benali Khodja M., Metouchi A., Djoudar Hallal D., Khelfi M.E.A., Önsoy H., Toumi S. 2022. Spatiotemporal characterization of the annual rainfall variability in the Isser Watershed (Algeria). Arabian Journal of Geosciences, 15, 2, 190. https://doi.org/10.1007/s12517-021-09408-x

Bénina T., Souhila I., Arezki O.A. 2006. Couplage d'une analyse en composantes principales et d'une approche géostatistique pour l'élaboration de cartes pluviométriques du Centre de l'Algérie du Nord. Revue des sciences de l'eau, 19,3, 213–219. https://doi.org/10.7202/013539ar

Bostan P. A., Heuvelink G.B.M., Akyurek S.Z. 2012. Comparison of regression and kriging techniques for mapping the average annual precipitation of Turkey. International Journal of Applied Earth Observation and Geoinformation, 19, 115–126. https://doi.org/10.1016/j.jag.2012.04.010

Boutouatou F. 2020. Les barrages en exploitation dans l'est algérien: fonctionnement hydrologique et aménagement. Etude de cas [Thèse Doctorat LMD]. Université Constantine 1.

Capot-Rey R. 1946. Études récentes sur le climat de l'Afrique du Nord et du Sahara. Annales de Géographie, 55, 297, 39–48. https://doi.org/10.3406/geo.1946.12714

Chaumont Paquin C. 1971. Carte pluviométrique de l'Algérie du Nord, échelle 1/500 000 (4 feuilles et notice. Société de l'Histoire Naturelle d'Afrique du Nord), Alger.

Chutsagulprom N., Chaisee K., Wongsaijai B., Inkeaw P., Oonariya C. 2022. Spatial interpolation methods for estimating monthly rainfall distribution in Thailand. Theor. Appl. Climatol., 148, 317–328. https://doi.org/10.1007/s00704-022-03927-7

Fellag M., Achite M., Wałęga A. 2021. Spatial-temporal characterization of meteorological drought using the standardized precipitation index. Case study in Algeria. Acta Scientiarum Polonorum, series Formatio Circumiectus, 20, 1, 19–31. https://doi.org/10.15576/ASP.FC/2021.20.1.19

Gaussen H. 1948. Carte des précipitations de l'Algérie (moyenne 1913–47, échelle 1/500 000 (4 feuilles) (Numéro elle 1/500 000). I.G.N.

Hallouz F., Meddi M., Mahé G., Ali Rahmani S., Karahacane H., Brahimi S. 2020. Analysis of meteorological drought sequences at various timescales in semi-arid climate: Case of the Cheliff watershed (northwest of Algeria). Arabian Journal of Geosciences, 13, 6, 280. https://doi.org/10.1007/s12517-020-5256-5

Karl T.R., Williams Jr. C.N. 1987. An Approach to Adjusting Climatological Time Series for Discontinuous In-TACT > 2.0.C homogeneities. Journal of Climate & Applied Meteorology, 26, 1744–1763.

Laborde J.-P. 1982. Cartographie automatique des caractéristiques pluviométriques: Prise en compte des relations pluviométrie-morphométrie. La Houille Blanche, 68, 4, 331–338. https://doi.org/10.1051/lhb/1982026

Laborde J.-P. 1995. Les différentes étapes d'une cartographie automatique: Exemple de la carte pluviométrique de l'Algérie du Nord. Publications de l'Association Internationale de Climatologie, 8, 37–46.

Laborde J.-P., Assaba M., Belhouli L. 2003. Les chroniques mensuelles de pluies de bassin: un préalable à l'étude des écoulements en Algérie. Colloque SHF „Gestion du risque eau en pays semi-aride", 21 mai 2023.

Laborde J.-P., Mouhous N., Assaba M. 2018. Mode d'utilisation du logiciel hydrolab 2018. Ecole polytechnique de l'université de Nice, Sophia Antipolis. http://www.legalis.net/cgiiddn/ certificat.cgi?IDDN.FR.010.0075748.000.R.C.1999.027.20700

Le Mezo L. 2013. Caractérisations agro-climatiques et estimation des besoins en eau d'irrigation: dans le cadre de l'Étude des modalités d'alimentation en eau brute du Cirque de Salazie. Cirad – Agritrop. https://agritrop.cirad.fr/568986/

Louamri A. 2009. Cartographie des pluies annuelles dans le bassin-versant de l'oued Seybouse (nord-est Algérien). Sciences & Technologie D, Sciences de la terre, 30, 43–52.

Mebarki A. 2003. Cartographie automatique des précipitations: Application à l'Est Algérien. Sciences & Technologie. B, Sciences de l'ingénieur, 100–107.

Mebarki A. 2010. Apport des cours d'eau et cartographie du bilan hydrologique: Cas des bassins de l'Algérie orientale. Science et changements planétaires/Sécheresse, 21, 4, 301–308.

Mebarki A., Assaba M., Laborde J.-P., Rezak S. 2013. Du bilan hydrologique au bilan hydrique: Modélisation et synthèse cartographique sur l'Algérie du Nord. Le 5e Colloque International sur Ressources en Eau et Développement Durable (CIREDD) Proceedings, 412–416.

Meddi H., Meddi M., Mahr N., Humbert J. 2014. Quantification of Precipitation: Application of Pluvia Method in the Northwest of Algeria. Production. In: Quantification Des Précipitations: Application Au Nord Ouest De L'Algérie-La Méthode Pluvia/Quantification of Precipitation: Application of Pluvia Method in the Northwest of Algeria. Production.

Merabti A. 2018. Caractérisation, variabilité et prévision de la sécheresse dans le Nord-Est Algérien [Thèse Doctorat]. ENSH, Blida, Algérie.

Mirgol B., Dieppois B., Northey J., Eden J., Jarlan L., Tramblay Y., Mahé G. 2022. Recent changes in the probability of agrometeorological risks over the southern Mediterranean region, and potential impacts on crop growth, 160. Display. https://doi.org/10.5194/egusphere-egu22-8677

ONID. 2020. Bilan d'exploitation 2020. Office National d'Irrigation et de Drainage. Direction Régionale du Chéliff. Unité Haut Chéliff (Algérie).

Seltzer P. 1946. Le climat de l'Algérie. Alger, Institut de Météorologie et de Physique du Globe. Carbonnel.

Surfer®. 2023. Golden Software L.L.C. www.goldensoftware.com

Taibi S., Meddi M., Souag D., Mahe G. 2013. Evolution et régionalisation des précipitations au nord de l'Algérie (1936–2009). Proceedings of H01, IAHS-IAPSO-IASPEI Assembly, 191–195.

Taibi S., Meddi M., Mahé G., Assani A. 2017. Relationships between atmospheric circulation indices and rainfall in Northern Algeria and comparison of observed and RCM-generated rainfall. Theoretical and Applied Climatology, 127, 1–2, 241–257. https://doi.org/10.1007/s00704-015-1626-4

Traboulsi M. 2010. La pluviométrie moyenne annuelle au Liban interpolation et cartographie automatique. Lebanese Science Journal, 11, 2, 11–25.

Tramblay Y., El Adlouni S., Servat E. 2013. Trends and variability in extreme precipitation indices over Maghreb countries. Natural Hazards and Earth System Sciences, 13, 12, 3235-3248. https://doi.org/10.5194/nhess-13-3235-2013

Van Nieuwenhuizen N., Lindsay J.B., DeVries B. 2021. Smoothing of digital elevation models and the alteration of overland flow path length distributions. Hydrological Processes, 35, 7. https://doi.org/10.1002/hyp.14271

Willmott C.J., Matsuura K. 2006. On the use of dimensioned measures of error to evaluate the performance of spatial interpolators. International Journal of Geographical Information Science, 20(1), 89–102. https://doi.org/10.1080/13658810500286976

Zahar Y., Laborde J.-P. 2008. Modélisation statistique et synthèse cartographique des précipitations journalières extrêmes de Tunisie. Revue des sciences de l'eau, 20, 4, 409–424. https://doi.org/10.7202/016914ar

Zerouali B., Chettih M., Abda Z., Mesbah M., Santos C.A.G., Brasil Neto R.M., Da Silva R.M. 2021. Spatiotemporal meteorological drought assessment in a humid Mediterranean region: Case study of the Oued Sebaou basin (northern central Algeria). Natural Hazards, 108, 1, 689–709. https://doi.org/10.1007/s11069-021-04701-0

Zerouali B., Elbeltagi A., Al-Ansari N., Abda Z., Chettih M., Santos C.A.G., Boukhari S., Araibia A.S. 2022. Improving the visualization of rainfall trends using various innovative trend methodologies with time-frequency-based methods. Appl. Water Sci., 12, 207. https://doi.org/10.1007/s13201-022-01722-3